Ultracold Dense Samples of Dipolar RbCs Molecules in the Rovibrational and Hyperfine Ground State

Tetsu Takekoshi,[1,2] Lukas Reichsöllner,[1] Andreas Schindewolf,[1] Jeremy M. Hutson,[3] C. Ruth Le Sueur,[3]
Olivier Dulieu,[4] Francesca Ferlaino,[1] Rudolf Grimm,[1,2] and Hanns-Christoph Nägerl[1]

[1]*Institut für Experimentalphysik, Universität Innsbruck, 6020 Innsbruck, Austria*
[2]*Institut für Quantenoptik und Quanteninformation, Österreichische Akademie der Wissenschaften, 6020 Innsbruck, Austria*
[3]*Joint Quantum Centre (JQC) Durham/Newcastle, Department of Chemistry, Durham University, South Road,
Durham DH1 3LE, United Kingdom*
[4]*Laboratoire Aimé Cotton, CNRS, Université Paris-Sud, Bâtiment 505, 91405 Orsay Cedex, France*

We produce ultracold dense trapped samples of ^{87}Rb^{133}Cs molecules in their rovibrational ground state, with full nuclear hyperfine state control, by stimulated Raman adiabatic passage (STIRAP) with efficiencies of 90%. We observe the onset of hyperfine-changing collisions when the magnetic field is ramped so that the molecules are no longer in the hyperfine ground state. A strong quadratic shift of the transition frequencies as a function of applied electric field shows the strongly dipolar character of the RbCs ground-state molecule. Our results open up the prospect of realizing stable bosonic dipolar quantum gases with ultracold molecules.

PACS numbers: 67.85.-d, 05.30.Rt, 33.20.-t, 42.62.Fi

Samples of ultracold molecules with dipole moments that can be tuned with applied electric fields offer a platform for exploring many new areas of physics. They are good candidates to form many-body systems with features such as supersolidity, unconventional forms of superfluidity, and novel types of quantum magnetism [1–3]. They allow exquisite control over all quantum degrees of freedom and offer the possibility of implementing quantum simulation protocols [4] that require genuine long-range interactions.

The most advanced experiments with ultracold polar molecules to date have been on KRb. Ni *et al.* [5] produced ultracold ^{40}K^{87}Rb molecules in states very close to dissociation by tuning a magnetic field across a Feshbach resonance and transferred the resulting Feshbach molecules to the rovibrational absolute ground state by stimulated Raman adiabatic passage (STIRAP). Similar work has been carried out on nondipolar Cs$_2$ [6,7]. The ground-state KRb molecules can be transferred between hyperfine states using microwave radiation [8] and confined in one-dimensional [9] and three-dimensional [10] optical lattices. However, pairs of KRb molecules can undergo an exothermic chemical reaction to form K$_2$ + Rb$_2$; this provides an opportunity for studies of quantum-state-controlled reactions [8,9,11] but also constitutes a loss mechanism for the trapped molecules.

There is great interest in producing samples of ultracold dipolar molecules that are collisionally stable. Żuchowski and Hutson [12] have shown that the molecules NaK, NaRb, NaCs, KCs, and RbCs in their absolute ground states are stable to all possible two-body collision processes. We have previously demonstrated that ^{87}Rb^{133}Cs Feshbach molecules can be produced from ultracold atoms

by magnetoassociation [13,14]. Similar work has been reported by Köppinger *et al.* [15]. In this Letter, we describe the transfer of these molecules to their rovibrational ground state by STIRAP. We also demonstrate magnetic control and show that the resulting molecules decay much more slowly when they are in their hyperfine ground state than when they are in an excited hyperfine state.

The states and transitions involved in our ground-state molecule production process are shown in Figs. 1(a)–1(c). A pump laser beam L$_p$ at 1557 nm couples a Feshbach state $|i\rangle$ with mostly $a^3\Sigma^+$ character to the $|v'=29\rangle$ level of the $b^3\Pi_1$ state with Rabi frequency Ω_p. This state has a small admixture of the $A^1\Sigma^+$ state [13] (Supplemental Material [16]), and a dump laser beam L$_d$ at 977 nm couples it to the rovibrational ground-state level $|v''=0, J''=0\rangle$ of the $X^1\Sigma^+$ potential with Rabi frequency Ω_d. This level is made up of 32 Zeeman sublevels, as shown in Fig. 1(c) [26]. At magnetic field $B=0$ the levels are grouped according to the total molecular nuclear spin $I''=2, 3, 4,$ or 5. The stretched state with $M_{I''} = M_{\text{tot}} = 5$ is the absolute ground state for B larger than about 90 G. It can be accessed at $B=181$ G using crossed vertical and horizontal linear polarizations (v$_p$, h$_d$) for L$_p$ and L$_d$ copropagating in the horizontal plane.

We start by generating a sample of ^{87}Rb^{133}Cs Feshbach molecules via magnetoassociation in an ultracold, magnetically levitated and nearly quantum-degenerate mixture of Rb and Cs atoms. The molecules are initially produced using the Feshbach resonance at $B=197.06$ G and then transferred by magnetic field ramps to the state $|-2(1,3)d(0,3)\rangle$ near $B=180$ G as sketched in Fig. 1(b) and described in more detail in Ref. [14]. Here, states are labeled with
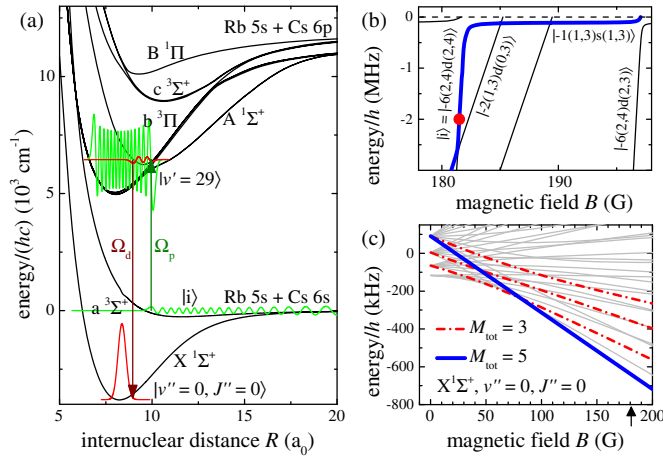
FIG. 1 (color online). STIRAP scheme and levels involved. (a) Ground- and excited-state molecular potentials of the RbCs molecule [13]. The transfer from the Feshbach state $|i\rangle$ at threshold to the rovibrational ground-state level $|v''=0, J''=0\rangle$ involves the $v'=29$ level belonging to the $b^3\Pi_1$ electronically excited state. The red and green solid lines indicate the wave functions that are coupled by the STIRAP pump and dump lasers L_p and L_d with Rabi frequencies Ω_p and Ω_d. (b) Zeeman diagram for the states with $M_{tot}=4$ just below the ground-state two-atom $(f_{Rb}, f_{Cs}) = (1, 3)$ threshold. The red dot marks the position from which STIRAP takes place. The magnetoassociation path is marked with a blue line. Energies are given relative to the field-dependent atomic dissociation threshold. (c) Zeeman diagram showing the ground-state hyperfine structure (32 states). The magnetic field during STIRAP is indicated by the arrow. The energy levels are calculated using the Hamiltonian and parameters from Ref. [27]. The thick lines show the final states allowed by the selection rule $\Delta M_{tot} = \pm 1$ for vertical pump and horizontal dump polarization (v$_p$, h$_d$).

quantum numbers $|n(f_{Rb}, f_{Cs})L(m_{f_{Rb}}, m_{f_{Cs}})\rangle$, where n is the vibrational quantum number counted downwards from the (f_{Rb}, f_{Cs}) dissociation threshold, f indicates the atomic total angular momentum with projection m_f, and L is the molecular rotational angular momentum. We take the quantization axis to lie along the magnetic field direction, which is vertical in our setup (Supplemental Material [16]).

The high-field-seeking molecules in state $|-2(1,3)d(0,3)\rangle$ are separated from the remaining atoms by the Stern-Gerlach effect. The magnetic field B is then ramped back up through the nearest avoided crossing to transfer the molecules into the strongly low-field-seeking state $|i\rangle = |-6(2,4)d(2,4)\rangle$ at a binding energy of approximately 2 MHz $\times h$ at $B = 181$ G (marked with a dot in Fig. 1(b)). This state is chosen because it has the greatest triplet fraction and the largest amplitude at short range, giving the most favorable Franck-Condon overlap for the STIRAP process described below. To reduce spatial Zeeman broadening and gravitational sag, the field gradient used for levitation is turned off and a vertical one-dimensional optical lattice (Supplemental Material [16]) is superimposed on the molecular cloud to hold it against gravity.

The molecular sample is, thus, held in a stack of pancake-shaped two-dimensional traps with their tight axis along the vertical direction. This additional step, combined with the shorter collisional lifetime of molecules in the $n = -6$ state (about 30 ms), reduces the cloud population from 3000 to between 1000 and 1500 trapped molecules with a $1/e^2$-cloud radius of between 30 and 40 μm. The translational temperature measured in expansion after sudden release from the trap is 240(30) nK. The overall sample preparation procedure takes about 13 s.

STIRAP is based on a pulse sequence in which the dump laser is turned on before the pump laser to generate a transient dark superposition of the initial and final states [28]. We perform ground-state STIRAP from $|i\rangle$ to $|v''=0, J''=0\rangle$ and characterize its efficiency by reversing the STIRAP process as shown in Fig. 2 [29]. Molecules are transferred to the hyperfine-Zeeman ground state with $M_{tot} = 5$ between $t \approx 15$ and 30 μs and back to the Feshbach state $|i\rangle$ between $t \approx 40$ and 55 μs. Both lasers are tuned to one-photon resonance for fixed $B = 181$ G. The Feshbach molecules are then detected by dissociating them at the Feshbach resonance at 197.06 G and using absorption imaging on the atomic clouds [14]. The round-trip transfer efficiencies are typically about 80%, implying one-way transfer efficiencies of about 90%. For comparison, the solid line in Fig. 2(a) is the result of a simulation that takes laser linewidth into account, but not beam shape and laser noise pedestal effects (Supplemental Material [16]). It gives a somewhat higher efficiency.

Scanning the dump laser detuning Δ_d reveals hyperfine and Zeeman substructure of the $X^1\Sigma^+$, $|v''=0, J''=0\rangle$
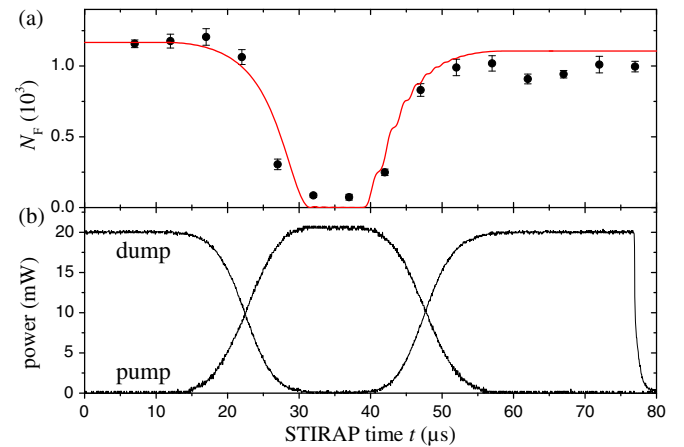

FIG. 2 (color online). Efficient ground-state STIRAP transfer. (a) Number of Feshbach molecules N_F as a function of STIRAP time t during a typical forward and reverse on-resonance STIRAP pulse sequence as shown in (b). The peak Rabi frequencies are $\Omega_p = 2\pi \times 0.77(22)$ MHz and $\Omega_d = 2\pi \times 2.3(6)$ MHz. The one-way STIRAP efficiency is 90%. The red curve is the result of a master equation model (Supplemental Material [16]). Error bars denote the 1σ standard statistical error. (b) Laser power as a function of time t as recorded by photodiodes.

state as shown in Fig. 3. For (v_p, h_d) polarization, the transfer is mostly into the level with $M_{tot} = 5$. For (v_p, v_d) polarization, the transfer is primarily into one of the two hyperfine-excited levels with $M_{tot} = 4$. The most important terms in the ground-state hyperfine Hamiltonian [27] are the nuclear Zeeman shift and the scalar nuclear spin-spin interaction, which are governed by the electronic and nuclear g factors, and the nuclear spin-spin parameter c_4, respectively. The second of these two terms dominates at low field. The g factors are very precisely known, and a simulation (Supplemental Material [16]) using them and the c_4 parameter of Ref. [27] agrees well with the observed spectrum for both choices of polarization.

There are usually 50 to 100 Feshbach molecules that remain after the transfer to the ground state [offset in Figs. 2(a) and 3]. We believe this is mainly due to a slight beam misalignment and the fact that the molecular cloud and STIRAP beams have similar radii. We exclude these molecules when calculating the transfer efficiency. The efficiency is most likely limited by laser power, in the sense that Feshbach molecules at the edge of the cloud see lower laser intensities. Laser phase noise pedestals may also play a role, as discussed in Ref. [30].

To explore the molecules' collisional properties, we load our sample of ground-state molecules into a three-dimensional
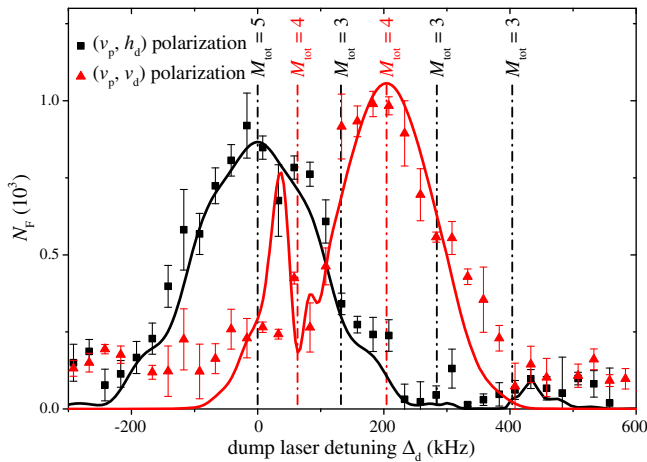
crossed dipole trap (Supplemental Material [16]). The trap is comparatively stiff with a geometrically averaged trap frequency of 409(20) Hz to hold the sample against gravity. The sample's peak particle density is now $1.1(1) \times 10^{11}$ cm^{-3}. The compression of the sample leads to a marked increase in temperature to 8.7(7) μK. Nevertheless, we expect that s-wave collisions dominate the collision process at zero electric field. Figure 4 shows the ground-state population in the $M_{tot} = 5$ state as a function of hold time t_h between forward and reverse STIRAP transfer for various values of the magnetic field B. For this measurement, we first prepare the molecular sample as before at $B = 181$ G in $M_{tot} = 5$ and then ramp the magnetic field to the chosen value within about 1 ms. After time t_h, we reverse the process and determine the remaining number of molecules. The results show ground-state molecule loss that depends strongly on B. Using a two-body decay model (Supplemental Material [16]), we determine the two-body loss rate coefficient L_2. Its dependence on B is shown in the inset to Fig. 4. The value of L_2 is considerably greater at fields below about 90 G. The state with $M_{tot} = 5$ is not the absolute ground state at fields below this threshold, as seen in Fig. 1(c), and we attribute the greatly reduced lifetime to hyperfine-changing collisions to form the lower-energy states. We note that L_2 is nonzero even for fields above 90 G; this may be due to thermal population of excited hyperfine states or to losses involving long-lived collision complexes [31,32]. We also note that our ground-state sample is not 100% pure,
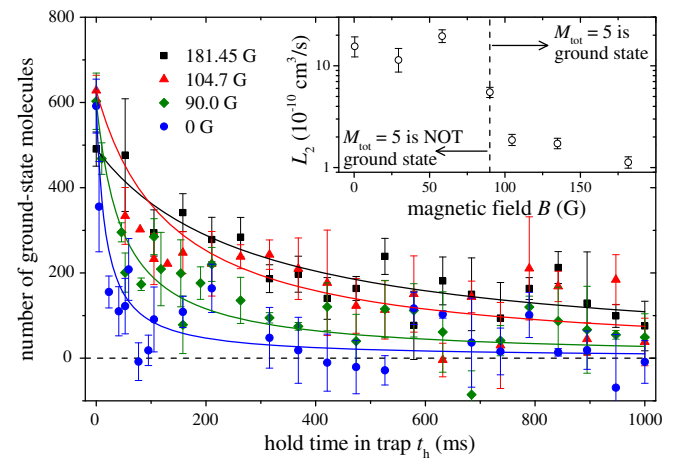

FIG. 3 (color online).   STIRAP spectrum showing the number of Feshbach molecules N_F after round-trip STIRAP as a function of dump laser detuning Δ_d for two different choices of the polarization of the dump laser. The energies of the hyperfine components of the ground state (calculated using the parameters of Ref. [27]) are marked with dashed vertical lines and labeled with their total angular momentum projection M_{tot}. For (v_p, h_d) polarization (black squares), the Feshbach molecules ($M_{tot} = 4$) are primarily transferred into the absolute hyperfine ground state with $M_{tot} = 5$. For (v_p, v_d) polarization (red triangles), hyperfine-excited levels are addressed. The solid curves are master equation simulation results (Supplemental Material [16]). The black curve centered around zero detuning is a fit to the data to determine the dump Rabi frequency. The Rabi frequencies are $\Omega_p = 2\pi \times 0.26(7)$ MHz and $\Omega_d = 2\pi \times 2.3(6)$ MHz.

FIG. 4 (color online).   Decay of ground-state molecules as a result of collisions at zero electric field. The number of ground-state molecules in $M_{tot} = 5$ is plotted against hold time t_h in the crossed dipole trap for different values of the magnetic field B as indicated. The initial peak density is $1.1(1) \times 10^{11}$ cm^{-3}. The solid lines are fits based on a two-body decay model to determine the two-body loss rate coefficient L_2 (Supplemental Material [16]). The fits are constrained to run through the first data point at zero hold time. The inset plots L_2 as a function of B. A greatly reduced L_2 is seen at magnetic fields B greater than about 90 G, where the molecules are mostly in the hyperfine-Zeeman ground state.
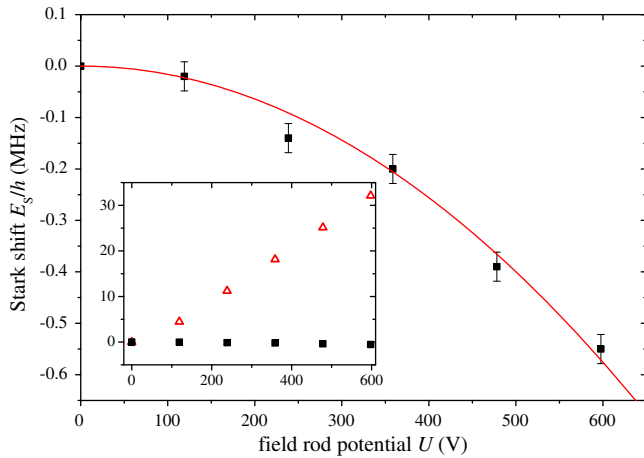
FIG. 5 (color online). Stark shift of the $M_{tot} = 5$ state of the RbCs ground state. The two-photon STIRAP resonance shift E_S is plotted as a function of the electrode potential U. The solid line is a quadratic fit. The inset shows an expanded range in which the excited-state shift can be seen as well (triangles).

because it initially contains some molecules left behind in the Feshbach state $|i\rangle$. The cross section for inelastic collisions between molecules in states $|M_{tot} = 5\rangle$ and $|i\rangle$ is likely to be large and will lead to some loss of ground-state molecules on the time scales considered here.

A crucial property of RbCs molecules is their permanent electric dipole moment μ, calculated to be 1.25 D in the absolute ground state [33,34]. We have measured the Stark shift of the hyperfine ground state by applying voltages to a set of four parallel electrodes external to the fused silica cell vacuum chamber [16] and tracking the shift E_S of the $M_{tot} = 5$ peak position (as in Fig. 3) from that recorded at zero electrode potential. The potential is pulsed to reduce charging effects from the alkali-coated cell walls (Supplemental Material [16]) [35]. The resulting shift is shown in Fig. 5. Both the dump and the pump laser must be detuned considerably, because of the large excited-state shift shown in the inset of Fig. 5. The quadratic shift is observed to be 1.60(7) Hz/V^2, which implies a permanent dipole moment of 1.17(2)(4) D. Here, the first error is statistical and the second is the estimated systematic error due to geometrical uncertainty that enters when calculating the dielectrically enhanced electric field inside our quartz cell apparatus (Supplemental Material [16]).

In conclusion, we have formed dense samples of ultra-cold RbCs molecules in their electronic and rovibrational ground state. The molecules are initially formed in near-dissociation states by magnetoassociation and transferred to the ground state by the STIRAP method. The efficiency of the ground-state transfer is about 90%. With an appropriate choice of laser polarization, we can produce the molecules in their absolute hyperfine ground state. RbCs molecules in their ground state are stable to all possible two-body collision processes, so our results offer the prospect of producing the first collisionally stable quantum gas of dipolar molecules.

In future work, we will attempt to increase the sample size and density by creating Feshbach molecules from atomic Mott insulators in a three-dimensional optical lattice [36], in generalization of work on homonuclear Cs_2 [7]. The dynamics will then be dominated by nearest-neighbor interactions with interaction strength on the order of $h \times 1$ kHz. This will allow us to study important problems in quantum many-body physics, such as the phase diagram of the Bose-Hubbard model extended by a long-range interaction term [37,38].

[1] C. Trefzger, C. Menotti, B. Capogrosso-Sansone, and M. Lewenstein, J. Phys. B **44**, 193001 (2011).

[2] M. Baranov, M. Dalmonte, G. Pupillo, and P. Zoller, Chem. Rev. **112**, 5012 (2012).

[3] T. Lahaye, C. Menotti, L. Santos, M. Lewenstein, and T. Pfau, Rep. Prog. Phys. **72**, 126401 (2009).

[4] I. Bloch, J. Dalibard, and S. Nascimbène, Nat. Phys. **8**, 267 (2012).

[5] K.-K. Ni, S. Ospelkaus, M. H. G. de Miranda, A. Pe'er, B. Neyenhuis, J. J. Zirbel, S. Kotochigova, P. S. Julienne, D. S. Jin, and J. Ye, Science **322**, 231 (2008).

[6] J. G. Danzl, E. Haller, M. Gustavsson, M. J. Mark, R. Hart, N. Bouloufa, O. Dulieu, H. Ritsch, and H.-C. Nägerl, Science **321**, 1062 (2008).

[7] J. G. Danzl, M. J. Mark, E. Haller, M. Gustavsson, R. Hart, J. Aldegunde, J. M. Hutson, and H.-C. Nägerl, Nat. Phys. **6**, 265 (2010).

[8] S. Ospelkaus, K.-K. Ni, G. Quéméner, B. Neyenhuis, D. Wang, M. H. G. de Miranda, J. L. Bohn, J. Ye, and D. S. Jin, Phys. Rev. Lett. **104**, 030402 (2010).

[9] M. H. G. de Miranda, A. Chotia, B. Neyenhuis, D. Wang, G. Quéméner, S. Ospelkaus, J. L. Bohn, J. Ye, and D. S. Jin, Nat. Phys. **7**, 502 (2011).

[10] A. Chotia, B. Neyenhuis, S. A. Moses, B. Yan, J. P. Covey, M. Foss-Feig, A. M. Rey, D. S. Jin, and J. Ye, Phys. Rev. Lett. **108**, 080405 (2012).

[11] K.-K. Ni, S. Ospelkaus, D. Wang, G. Quemener, B. Neyenhuis, M. H. G. de Miranda, J. L. Bohn, J. Ye, and D. S. Jin, Nature (London) **464**, 1324 (2010).

[12] P. S. Żuchowski and J. M. Hutson, Phys. Rev. A **81**, 060703 (R) (2010).

[13] M. Debatin, T. Takekoshi, R. Rameshan, L. Reichsöllner, F. Ferlaino, R. Grimm, R. Vexiau, N. Bouloufa, O. Dulieu, and H.-C. Nägerl, Phys. Chem. Chem. Phys. **13**, 18926 (2011).

[14] T. Takekoshi, M. Debatin, R. Rameshan, F. Ferlaino, R. Grimm, H.-C. Nägerl, C. R. Le Sueur, J. M. Hutson, P. S. Julienne, S. Kotochigova *et al.*, Phys. Rev. A **85**, 032506 (2012).

[15] M. P. Köppinger, D. J. McCarron, D. L. Jenkin, P. K. Molony, H.-W. Cho, S. L. Cornish, C. R. Le Sueur, C. L. Blackley, and J. M. Hutson, Phys. Rev. A **89**, 033604 (2014).

[16] See the Supplemental Material at http://link.aps.org/supplemental/10.1103/PhysRevLett.113.205301 for details on the molecular states, on laser light generation, on the optical lattice, on modeling the STIRAP time course, on the two-body decay model, and on the dc-Stark shift measurement setup, including Refs. [17–25].

[17] N. V. Vitanov and S. Stenholm, Opt. Commun. **135**, 394 (1997).

[18] B. W. Shore, J. Martin, M. P. Fewell, and K. Bergmann, Phys. Rev. A **52**, 566 (1995).

[19] J. Martin, B. W. Shore, and K. Bergmann, Phys. Rev. A **52**, 583 (1995).

[20] N. V. Vitanov and S. Stenholm, Phys. Rev. A **60**, 3820 (1999).

[21] O. Docenko, M. Tamanis, R. Ferber, T. Bergeman, S. Kotochigova, A. V. Stolyarov, A. de Faria Nogueira, and C. E. Fellows, Phys. Rev. A **81**, 042511 (2010).

[22] S. Kotochigova (private communication).

[23] T. Takekoshi, R. Grimm, and H.-C. Nägerl (to be published).

[24] J. Alnis, A. Matveev, N. Kolachevsky, T. Udem, and T. W. Hänsch, Phys. Rev. A **77**, 053809 (2008).

[25] C. W. Gardiner and P. Zoller, *Quantum Noise* (Springer, Berlin-Heidelberg, 2010).

[26] J. Aldegunde and J. M. Hutson, Phys. Rev. A **79**, 013401 (2009).

[27] J. Aldegunde, B. A. Rivington, P. S. Żuchowski, and J. M. Hutson, Phys. Rev. A **78**, 033434 (2008).

[28] K. Bergmann, H. Theuer, and B. W. Shore, Rev. Mod. Phys. **70**, 1003 (1998).

[29] M. Debatin, Ph.D. thesis, University of Innsbruck, 2013.

[30] L. P. Yatsenko, B. W. Shore, and K. Bergmann, Phys. Rev. A **89**, 013831 (2014).

[31] M. Mayle, G. Quéméner, B. P. Ruzic, and J. L. Bohn, Phys. Rev. A **87**, 012709 (2013).

[32] K. Lauber, E. Kirilov, M. J. Mark, F. Meinert, and H.-C. Nägerl (to be published).

[33] M. Aymar and O. Dulieu, J. Chem. Phys. **122**, 204302 (2005).

[34] S. Kotochigova and E. Tiesinga, J. Chem. Phys. **123**, 174304 (2005).

[35] M. A. Bouchiat, J. Guena, P. Jacquier, M. Lintz, and A. V. Papoyan, Appl. Phys. B **68**, 1109 (1999).

[36] A. Lercher, T. Takekoshi, M. Debatin, B. Schuster, R. Rameshan, F. Ferlaino, R. Grimm, and H.-C. Nägerl, Eur. Phys. J. D **65**, 3 (2011).

[37] B. Damski, L. Santos, E. Tiemann, M. Lewenstein, S. Kotochigova, P. Julienne, and P. Zoller, Phys. Rev. Lett. **90**, 110401 (2003).

[38] B. Capogrosso-Sansone, C. Trefzger, M. Lewenstein, P. Zoller, and G. Pupillo, Phys. Rev. Lett. **104**, 125301 (2010).